Electronic Supplementary Material (ESI) for Soft Matter.
This journal is © The Royal Society of Chemistry 2017

Supplementary Information for

Controlling the self-folding of a polymer sheet by a local heater: effect of the polymer-heater interface

*Jianxun Cui, Shanshan Yao, Qijin Huang, John Adams and Yong Zhu**

Department of Mechanical and Aerospace Engineering, North Carolina State University, Raleigh, North Carolina 27695-7910, USA

E-mail: yong_zhu@ncsu.edu

1. Failure of AgNW thin film directly coated on PS substrate

If the heater was fabricated by coating AgNW directly on top of PS, it tended to fail before folding occurs. This might be due to non-uniform heating of the PS. Hot spots can be generated where temperature was higher than the surrounding area. These hot spots shrank faster, thus generated local tensile strain on the surrounding area of PS substrate and the AgNW film on top, which lead to cracking of the AgNW film. Fig. S1 shows cracks in the AgNW film.

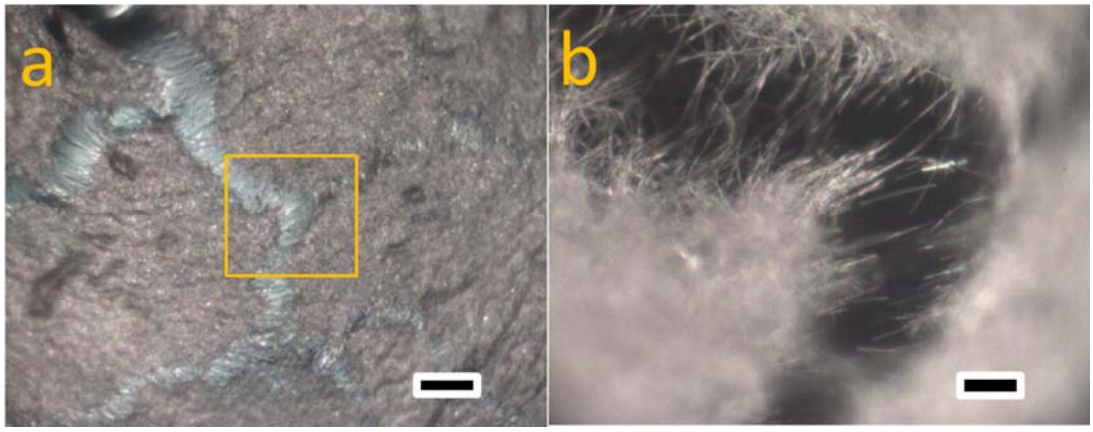

Fig. S1. Failure of a AgNW film heater on PS. (b) High magnification image of the highlighted region in (a). Scale bars: (a) 100 μm; (b) 20 μm.

2. Temperature characterization by IR camera

Heater temperature was characterized by a IR camera. Fig. S2a shows the temperature evolution of a heater when different input powers were applied. Constant current was applied for each power. With higher input power, higher equilibrium temperature was obtained. When current was turned off, the temperature decreased rapidly (decreased 20 degrees in less than 5 seconds). This explained why the folding can be stopped by turning off the current. The heater did not need to reach steady state to start the folding. With a high input power, it can reach the threshold temperature for shrinkage before reaching steady state.

Fig. S2b shows the IR images of PI heater at the corresponding input power of Fig. S2a. Heater appeared darker than the surrounding area (PS), which can be explained by working principle of the IR camera. IR camera measures radiance from the surface, which is determined by temperature and emissivity of the object. The color bar is based on the radiance. Brighter color corresponds to higher radiance. The emissivity is needed to get the correct temperature.[1] AgNW heater appeared colder in IR image. This is due to the ultralow emissivity of AgNW.[2] The emissivity value of AgNW was calibrated (~0.12). Fig. S3 shows the IR images of a heater during folding. The heater was bonded to PS with superglue. Outward folding (folding against heater) occured when temperature was about 140 degrees.

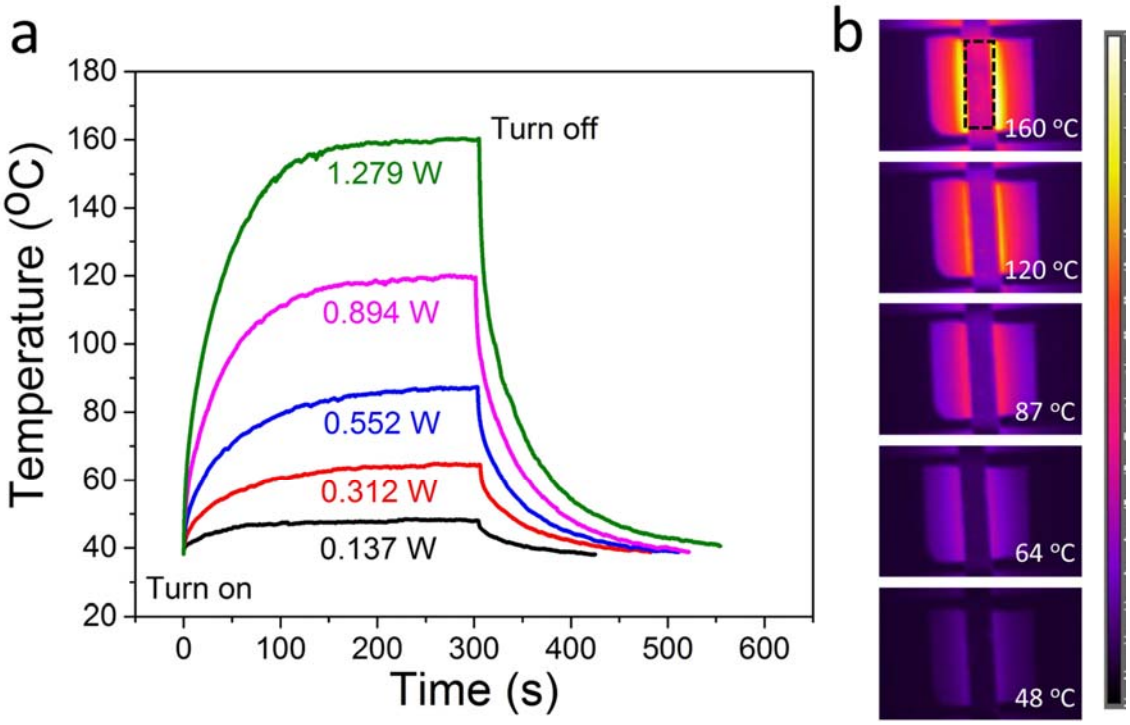

Fig. S2. Characterization of the heater using IR camera. (a) Temperature evolution of the heater at different input powers. (b) IR image of the heater at the corresponding input power of (a). The temperatures shown in (a) were the average temperatures in the area highlighted by the black dash line. A piece of PS without pre-strain was attached below the heater in order to replicate the condition for folding.

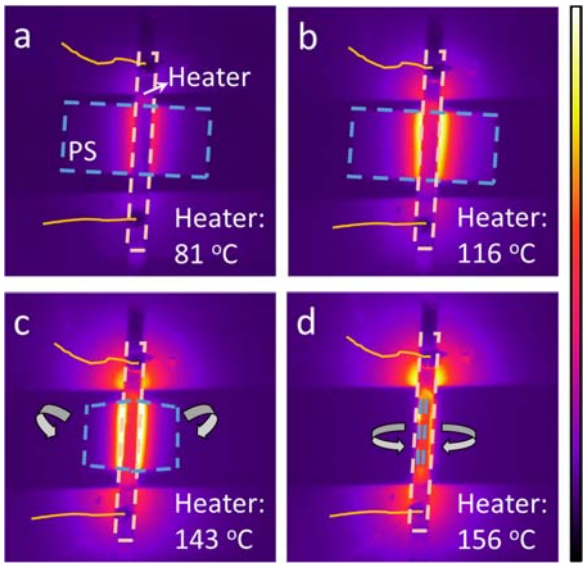

Fig. S3. IR image of a heater during outward folding. The heater is illustrated by yellow dash line and the PS sheet illustrated by blue dash line. PS sheet folded downwards.

3. Folding results without constraint

Fig. S4 shows inward folding with a 0.5 mm wide heater. Maximum folding angle was 140 degrees.

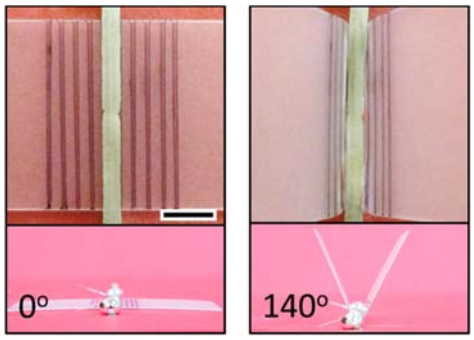

Fig. S4. Inward folding with a 0.5 mm wide heater. Scale bar: 2 mm.

4. Geometric calcultion of the heater climbing up process

Without constraint, heater tended to slide on PS to accommodate the folding. It cannot remain in conformal contact with PS during folding. Instead, the central part delaminated from PS while the edges slid along PS. This is shown schematically in Fig. S5a. The chord length was measured from the top view image (as the projected width of heater). From this chord length and the folding angle, the arc shape of PS beneath the heater can be determined (shown below). Note that central angle of the arc was equal to the folding angle. The shape of heater was also approximated by an arc, whose length was constant during folding. Once the arcs of PS and heater were determined, the displacement of the center relative to the edge can be determined. The gap between heater and PS (at the center of heater) was calculated and shown in Fig. S5b. The heater buckled considerably as a result of compression during the folding. The initial chord length was 2.3 mm, equal to the heater width. It was reduced to 2.13 mm when the heater was folded to 180 degrees. Initially, the heater and PS were in intimate contact. As folding continued, the gap between heater and PS increased. The gap at the center was 0.69 mm when PS was folded to 180 degrees.

Calculation of the arc shape from chord length and central angle is shown in Fig. S6. Central angle (α) is equal to folding angle. Chord length (l) was measured from the projected width of heater. Radius of curvature (R) can be calculated from Equation S1. It needs to be noted that the radius of curvature might be bigger than the ideal case, since shrinkage of top surface might be incomplete and bottom surface might also shrink.

$$\sin(\frac{\alpha}{2}) = \frac{l/2}{R} \qquad \text{(S1)}$$

The heater was also approximated by an arc. As shown in Fig. S7, the arc length (d) was equal to heater width measured from the initial configuration. Chord length (l) was measured from

the top view image. Radius (R') and central angle (α') can be calculated from Equations S2 and S3.

$$\sin(\frac{\alpha'}{2}) = \frac{l/2}{R'} \quad \text{(S2)}$$

$$\alpha' = \frac{d}{R'} \quad \text{(S3)}$$

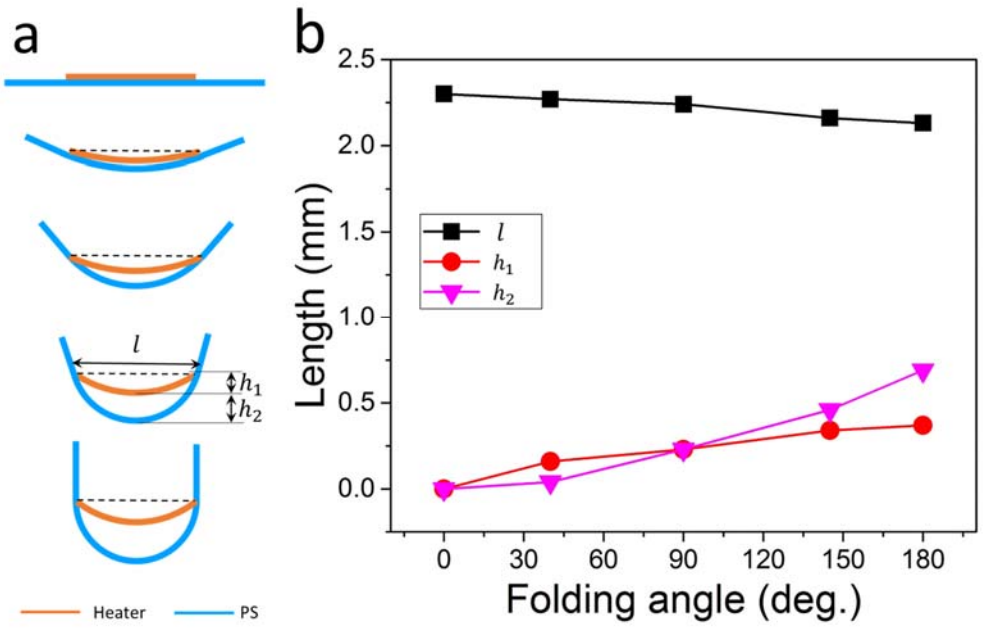

Fig. S5. Heater morphology during inward folding. (a) Schematics of cross sections of the heater on PS during folding. (b) The chord length and gaps between the heater and PS as a function of folding angle.

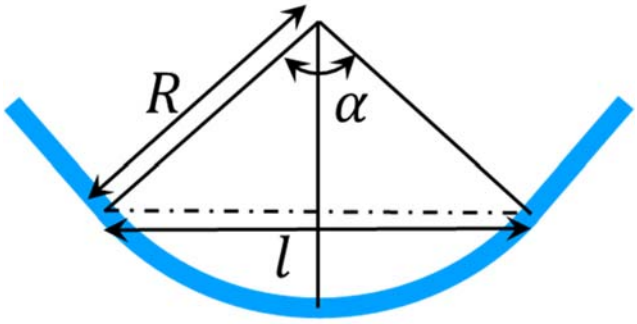

Fig. S6. Calculation of the arc from the chord length and central angle of the PS sheet.

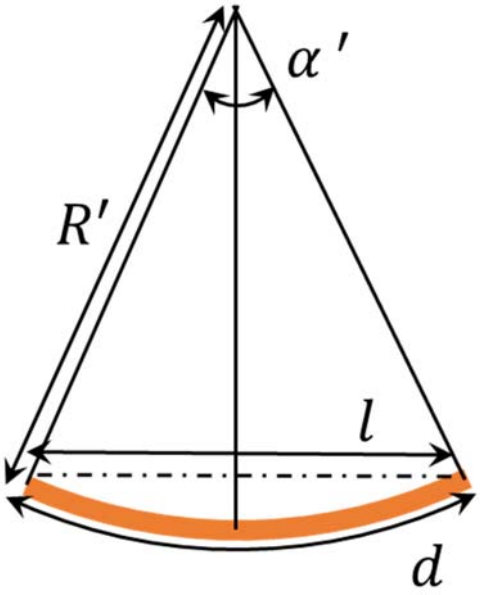

Fig. S7. Calculation of the arc from chord length and arc length of the heater.

5. Folding with partial constraint

Heater can be anchored at two edges by bare tapes. In this case, sliding of the heater was not allowed. However, delamination of heater can still occur due to the weak adhesion. Inward folding was supressed. Fig. S8 shows folding results with a 0.5 mm wide heater with both edges of the heater constrained.

The sliding of heater can be partly suppressed by using bare tape on one side of the heater. Fig. S9 shows the heater morphology during folding with the left edge ofthe heater constrained. Complete inward folding can be obtained in this case.

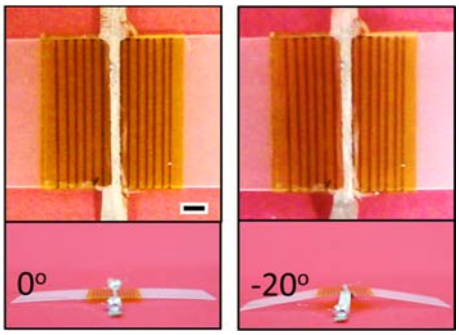

Fig. S8. Folding results with a 0.5 mm wide heater under patial constraint. Bare tape was applied on both edges to prevent sliding of the heater. Scale bar: 2 mm.

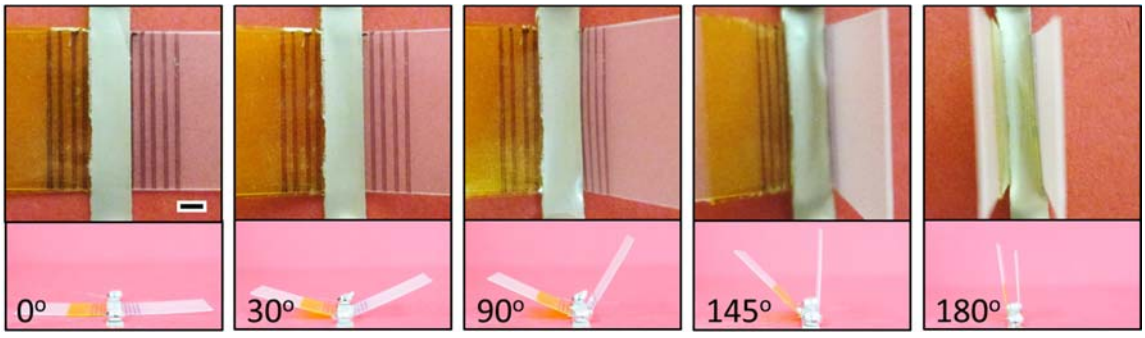

Fig. S9. Heater morphology during folding with bare tape on the left side to prevent sliding of the heater from left side. Scale bar: 2 mm.

6. Finite element modeling

To achieve outward folding, bottom side needs to be heated up. As heat transferred to the bottom side through the thickness, it also spread in plane laterally. Thus an area beyond the heater on top surface can be heated up. We call this extra heated area. We used finite element analysis (FEA) to model the steady state temperature distribution. ANSYS version 16.1 was used for the modeling. A constant temperature (155 ^{o}C) at heater position was applied. Convective boundary condition was applied to the rest area. Ambient temperature was set to 25 ^{o}C, and convective heat transfer coefficient was set to 30 $Wm^{-1}K^{-1}$. Table S1 lists the material constants used in the finite element model. Fig. S10 shows the temperature distributions across the PS for heaters with different widths. Extra heated area was found to be independent of the heater width, for a given PS thickness. But a wider heater can cause a wider area on bottom side to be heated up. This explained why narrow heater caused inward folding, while wide heater lead to outward folding (in the case of total constraint).

Transient FEA analysis was also performed to show the temperature evolution in the thickness direction as well as the lateral direction. Fig. S11 shows the temperature distribution across the PS sheet as a function of time for a 2 mm heater. Constant heat flux boundary condition was assumed at the heater-PS interface. Heat flux was 6900 Wm^{-2}. This corresponded to 0.17 W (heat flux times heating area of 24 mm^2) of Joule heating power. Steady-state temperature at the heater position was about 155 ^{o}C. From the transient analysis, the temperature across the PS layer approached steady state in about 25 seconds

Table S1. Material properties of PS used in finite element model.

Thermal conductivity	0.14 W m^{-1} K^{-1}
Density	1050 kg m^{-3}
Specific heat	1300 J kg^{-1} K^{-1}

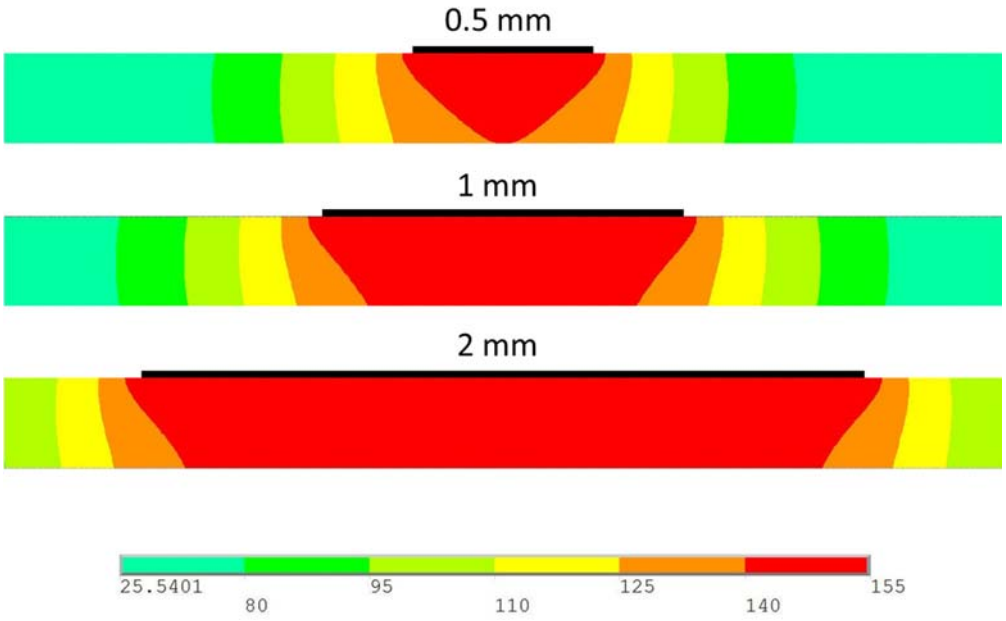

Fig. S10. Temperature distribution across the PS layer under the heater with different widths (FEA steady state analysis). The heater width is indicated by black line.

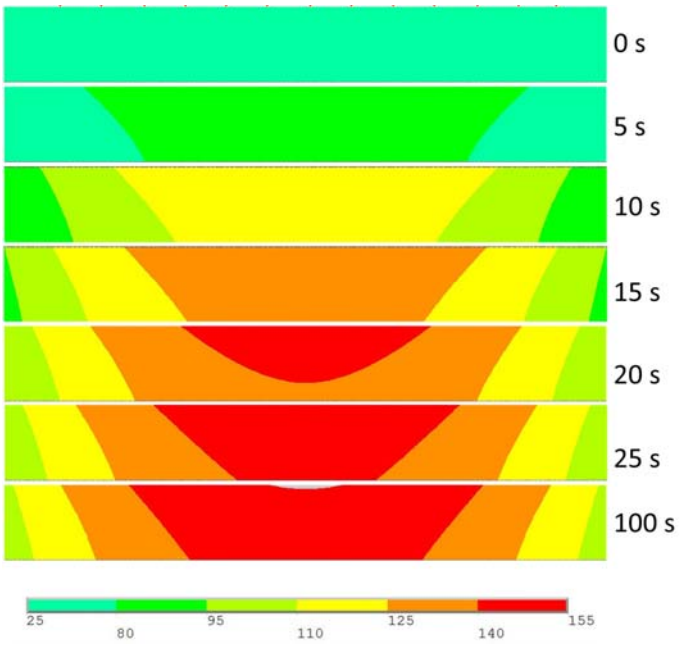

Fig. S11. Temperature evolution across the PS layer (FEA transient state analysis).

7. Folding results in the case of total constraint

Fig. S12 shows the folding results in the case of total constaint. 0.5 mm wide heater gave rise to inward folding, while 2 mm wide heater gave rise to complete outward folding.

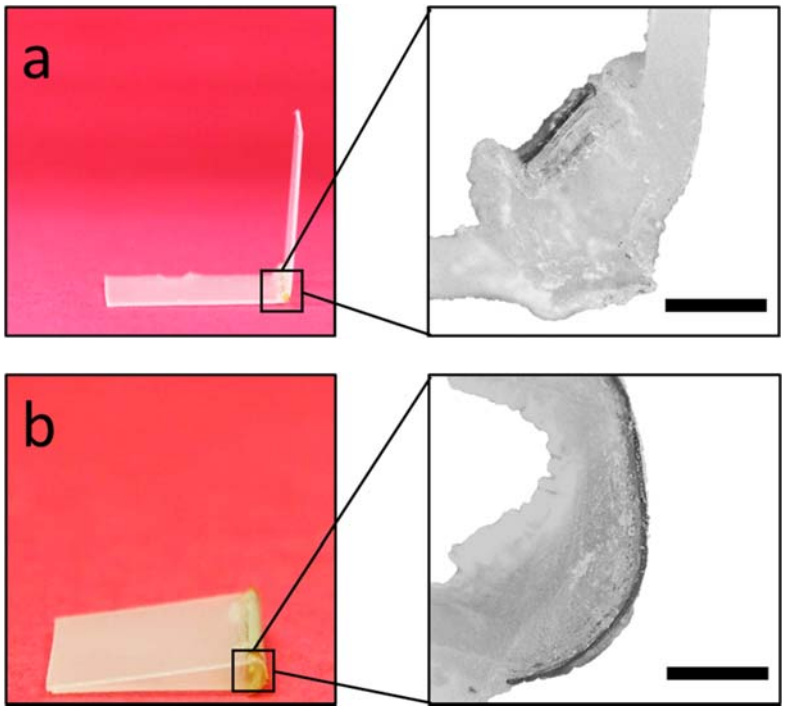

Fig. S12. Folding results in the case of total constraint. (a) Inward folding with a 0.5 mm wide heater. (b) Complete outward folding with a 2 mm wide heater. The inset in (a) and (b) shows optical microscopic images of the hinge region. Scale bars: 500 μm.

8. Bimorph model analysis

The outward folding when PI heater was bonded to PS using super glue was analyzed using bimorph model.[3] As shown in Fig. S13

, the blue layer is PS and yellow layer is PI. The thicknesses of the two layers are $h_1 = 0.025\ mm$ and $h_2 = 0.25\ mm$. The Young's modulus are $E_1 = 2000\ MPa$ and $E_2 = 1\ MPa$. Width (penpendicular to the page) w can be unit width.

The forces acting on the PI layer can be represented by an axial compressive force P_1 and a bending moment M_1. The forces acting on the PS layer can be represented by an axial tensile force P_2 and a bending moment M_2. The condition of equilibrium requires that:

$$P_1 = P_2 = P \tag{S4}$$

$$M_1 + M_2 = \frac{P_1 h_1}{2} + \frac{P_2 h_2}{2} \tag{S5}$$

Bending moment can be related to the in radius of curvature R:

$$M_1 = \frac{E_1 I_1}{R} \tag{S6}$$

$$M_2 = \frac{E_2 I_2}{R} \tag{S7}$$

The area moment of inertia can be calculated using the following formula:

$$I_1 = \frac{w h_1^3}{12} \tag{S8}$$

$$I_2 = \frac{w h_2^3}{12} \tag{S9}$$

Combine Equations (S4-S9) one can get the relationship between axial force and radius of curvature:

$$\frac{E_1 w h_1^3}{12R} + \frac{E_2 w h_2^3}{12R} = P\frac{h_1}{2} + P\frac{h_2}{2} \tag{S10}$$

Another equation can be obtained by considering that there is no sliding at the interface. Strain on both surface must be equal at the interface. Assume PS layer shrinks to 50% and there is no shrinkage or expansion in PI layer.

$$-50\% + \frac{P}{E_2 w h_2} + \frac{h_2}{2R} = -\frac{P}{E_1 w h_1} - \frac{h_1}{2R} \qquad \text{(S11)}$$

Substitutes in the materials properties and geometric parameters. The radius of curvature is calculated to be:

$$R = 0.504\ mm \qquad \text{(S12)}$$

This is similar to the results by assuming one surface cannot shrink while the other shrink freely to 50% (which corresponds to 0.5 mm radius of curvature). Based on the Equation 2 in the main text, the width required to be heated to achieve complete folding is

$$L = R\pi = 1.58\ mm \qquad \text{(S13)}$$

It needs to be noted that this is an oversimplified model, since it neglects the thickness of the bilayer when calculating the radius of curvature. However, it does show that the radius of curvature is quite small, which is comparable with the thickness of the bilayer structure. This analysis is similar to what has been reported in Bao's work.[4]

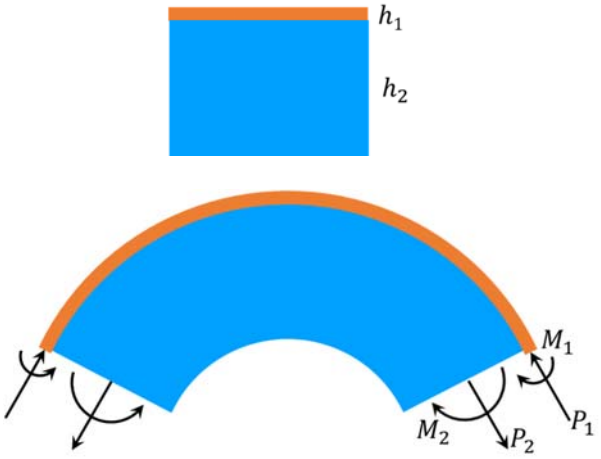

Fig. S13. Structure and force diagrams of the bilayer structure. Yellow layer: PI; blue layer: PS.

9. Repeatability of time response of folding

Fig. S14 shows the time responses of two additional samples for no constraint and total constraint folding. In the case of no constraint, the PS sheet folded to 180 degrees in about 38 s; while in the case of total constraint, folding finished in about 5 s

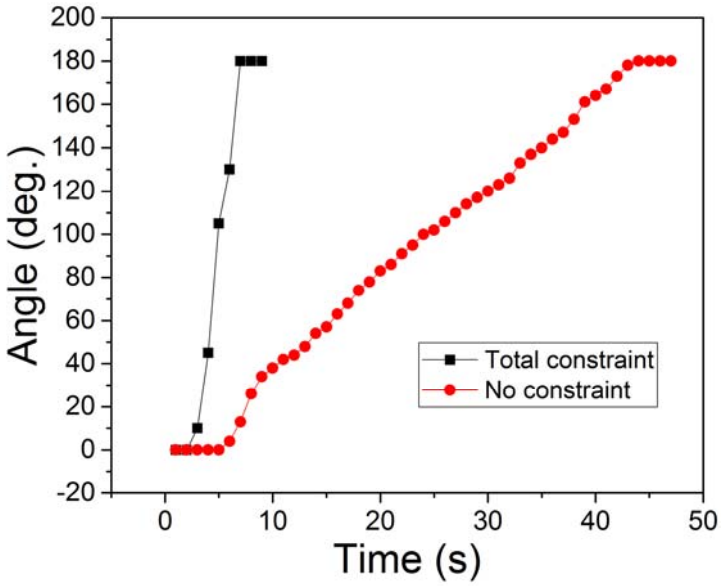

Fig. S14 Time responses of two additional samples in total constraint and no constraint modes

10. Video clips

Video S1. Folding process of digital number 6 (speed up to 13X faster).
Video S2. Folding process of a crane (speed up to 25X faster).

References:

1. R. P. Madding, 1999.
2. P.-C. Hsu, X. Liu, C. Liu, X. Xie, H. R. Lee, A. J. Welch, T. Zhao and Y. Cui, *Nano Lett.*, 2014, **15**, 365-371.
3. S. Timoshenko, *JOSA*, 1925, **11**, 233-255.
4. H. Wang, Y. Wang, B. C. K. Tee, K. Kim, J. Lopez, W. Cai and Z. Bao, *Adv. Sci.*, 2015, **2**, 1500103.